

Mean and Variance of Interference in Vehicular Networks with Hardcore Headway Distance

Konstantinos Koufos and Carl P. Dettmann

Abstract

Interference statistics in vehicular networks have long been studied using the Poisson Point Process (PPP) for the locations of vehicles. Under congested traffic, this model becomes unrealistic because it assumes that the vehicles can come arbitrarily close to each other. In this paper, we model the headway distance (the distance between the head of a vehicle and the head of its follower) equal to the sum of a constant hardcore distance and an exponentially distributed random variable. We investigate the impact of this model on the mean and the variance of interference at the origin in comparison with a PPP model of equal intensity. Even though the pair correlation function becomes much more complex as compared to the PPP, we develop simple models to capture the impact of hardcore distance on the variance of interference. In addition, we study the extreme scenario where the interference originates from a lattice. We show how to relate the variance of interference due to a lattice to that of a PPP of half intensity under Rayleigh fading.

Index Terms

Headway model, interference model, stochastic geometry, vehicular networks.

I. INTRODUCTION

Interference statistics in wireless networks with unknown locations of users have long been studied using stochastic geometry [1]. Due to its analytical tractability, the Poisson Point Process (PPP) is perhaps the most commonly employed model. Non-homogeneous PPPs have been used to capture a variable intensity of users across the deployment domain, for instance due to mobility [2], [3] or population density variations. By definition, a PPP assumes that two points (or users) can come arbitrarily close

K. Koufos and C.P. Dettmann are with the School of Mathematics, University of Bristol, BS8 1TW, Bristol, UK. {K.Koufos, Carl.Dettmann}@bristol.ac.uk

This work was supported by the EPSRC grant number EP/N002458/1 for the project Spatially Embedded Networks.

to each other. This assumption may be inaccurate due to physical constraints [4] and/or medium access control [5]. In that case, repulsive points processes as used here might be more suitable for performance evaluation.

Vehicular networks are expected to play a key role in improving traffic efficiency and safety in the near future [6]. An accurate model of interference in vehicular networks requires taking into account deployment constraints due to the road infrastructure. Note that using a planar two-dimensional PPP to study the performance of vehicular networks along orthogonal streets is not accurate in the high reliability regime [7]. An accurate study requires combining two spatial models; one for the road network and another for the locations of vehicles along each road.

The Manhattan Poisson Line Process has been a popular model for the road infrastructure, where the resulting blocks might be filled in with buildings to resemble urban districts. In cellular networks, it has been shown that a user traveling on a street experiences discontinuous interference at the intersections [8]. In the absence of buildings, the interference from other roads can be mapped to interference from own road with a non-uniform density of users facilitating the analysis [9], [10]. Recently, the Poisson Line Process has also been studied to model the distribution of roads with random orientations [11], [12]. In an ad hoc setting, the intensities of roads and users have conflicting effects: Increasing the intensity of roads (while keeping fixed the intensity of vehicles per road) increases the interference while, increasing the intensity of vehicles reduces the average link distance of the typical transmitter-receiver pair and improves coverage [11].

A common assumption in [7]–[12] is that the locations of vehicles follow independent PPPs. Similar assumption has been adopted for performance analysis of vehicular networks over higher layers, e.g., the study in [13] optimizes jointly the transmission range and the transmission probability for maximizing transport capacity in linear networks with random access. There are some studies, e.g. [10], [14] using Matérn type of processes to approximate the density of simultaneous transmissions by vehicles under the repulsive nature of IEEE 802.11p. The parent density is still PPP. Finally, vehicular connectivity studies combining queueing theory with random geometric graphs often make a similar assumption for exponential distribution of inter-arrivals [15].

A great deal of transportation research since the early 1960's has recognized that the distribution of headway distance (the distance measured from the head of a vehicle to the head of its follower [16], or simply the inter-vehicle distance) is not exponential under all circumstances. Different models have been proposed to approximate the distribution of headway, with the accuracy of a particular model depending on the traffic status [17]. Empirical studies have shown that the distribution of time headway (time difference between successive vehicles as they pass a point on the roadway [16]) is well-approximated by the log-

normal distribution under free flow [18], [19] and log-logistic distribution under congested flow [17]. Due to the mixed traffic conditions, Cowan has proposed not only single (exponential, shifted-exponential), but also mixed distribution models to describe the distribution of headway [20].

To the best of our knowledge, apart from the exponential distribution, other headway distance models have not been incorporated into the performance analysis of vehicular networks with interference. In [21], the log-normal distribution for the headway distance along with Fenton-Wilkinson approximation for multi-hop distances is used to study the lifetime of a link. The randomness is due to mobility and headway distribution while fading and interference are neglected.

Given a fixed and constant one-dimensional intensity of users (or vehicles), the PPP assumes that their locations are independent, resulting to high interference variations at the origin, once averaged over the ensemble of all possible location realizations. The motivation for this paper is to investigate how the variance of interference behaves by introducing a more realistic deployment model. The simplest possible enhancement assumes that the headway distance is not exponentially distributed but it is equal to the sum of a constant hardcore distance (or tracking distance) and an exponentially distributed Random Variable (RV). The hardcore distance may model the average length of a vehicle under free flow traffic or the average length of a vehicle plus a safety distance under congested traffic, hence the name tracking distance. Since the hardcore distance is assumed to be fixed and constant, the distribution of headway distance becomes shifted-exponential.

The shifted-exponential (instead of exponential) distribution for the headway, makes the locations of vehicles correlated. The associated pair correlation function has been studied in the context of radial distribution function for hard spheres in statistical mechanics, see for instance [22], [23], and it has a complex form. The contributions of this paper are two-fold:

- For small hardcore distance c as compared to the mean inter-vehicle distance λ^{-1} , we show that the variance of interference at the origin can be approximated by the variance of interference due to a PPP of equal intensity λ scaled with $e^{-\lambda c}$. This model allows getting a quick insight on the impact of tracking distance on the variance under various traffic conditions.
- We study the variance of interference at the origin due to a linear lattice in order to shed some light on the behavior of the variance when the tracking distance becomes comparable to the mean inter-vehicle distance. Besides fading, the source of randomness in this set-up is the distance between the lattice points and the cell borders. We devise a simple, yet accurate, model approximating the interference under the assumptions of Rayleigh fading and small inter-point lattice distance as compared to the cell size.

The rest of the paper is organized as follows. In Section II, we present the system set-up and system

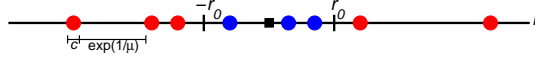


Fig. 1. The vehicles are modeled as identical impenetrable disks. The vehicles outside of the cell (red disks) generate interference to the base station (black square). The rest (blue disks) are associated to the base station and do not generate interference. In the figure, the tracking distance is illustrated to be equal to the diameter of the disk.

model assumptions. In Section III, we show how to calculate the mean and variance of interference in vehicular networks with hardcore distance. In Section IV, we derive closed-form approximations for the variance after simplifying the pair correlation function. In Section V, we study the extreme scenario where the interference originated from a lattice, approximating cases like platoons of vehicles and traffic jams. Finally, in Section VI, we conclude the paper and discuss relevant topics for future work.

II. SYSTEM MODEL

Let us assume that the headway distance between successive vehicles has two components: a constant tracking component $c > 0$ and a free component following the exponential distribution with mean μ^{-1} . This model degenerates to the time headway model M2 proposed by Cowan [20], if all the vehicles move with the same constant speed. We study interference at a single snapshot. The base station is located at the origin, and the vehicles located in the interval $[-r_0, r_0]$ are associated to it, not generating interference. The rest of the vehicles generate interference, see Fig. 1.

A valid uplink cellular network study requires us to incorporate power control, and also the constraint that a single vehicle per antenna sector transmits at a given time-frequency resource block, see for instance [24]. We leave a more explicit study of vehicular-to-infrastructure performance for future work. In this paper, we would like to get a preliminary insight into the impact of correlated user locations due to the tracking distance on the interference; incorporating all uplink modeling details would make the analysis much more involved considering the complex behavior of the pair correlation function, shortly to be seen in the next section.

Regarding channel modeling, the distance-based propagation pathloss model is $g(r) = r^{-\eta}$, where $\eta > 2$ stands for the propagation pathloss exponent. The fast fading h over each link is Rayleigh, and its impact on the interference power is modeled by an exponential RV with mean equal to unity, $\mathbb{E}\{h\} = 1$. The fading samples from different vehicles are independent RVs. Finally, the transmit power level is taken equal to unity.

III. MEAN AND VARIANCE OF INTERFERENCE

The mean interference at the origin can be calculated using the Campbell's Theorem [25]. Given the parameters μ, c of the deployment model, the intensity λ of vehicles is constant and equal to $\lambda^{-1} = c + \mu^{-1}$, or $\lambda = \frac{\mu}{1+c\mu}$ [20]. After averaging the distance-based propagation pathloss over the intensity of vehicles generating interference, we get the mean interference level equal to

$$\mathbb{E}\{\mathcal{I}\} = 2\lambda\mathbb{E}\{h\} \int_{r_0}^{\infty} g(r) dr = \frac{2\lambda r_0^{1-\eta}}{\eta-1}, \quad (1)$$

where the factor 2 comes from the vehicles located in the negative half-axis.

Equation (1) indicates that the tracking distance does not affect the mean interference while keeping the intensity of vehicles fixed. The mean interference due to a PPP of intensity λ is still given by (1). The second moment accepts contributions not only from a single vehicle but also from pairs of vehicles. Unlike the PPP, the locations of two vehicles become correlated with positive tracking distance. The second moment of interference is

$$\mathbb{E}\{\mathcal{I}^2\} = 2\lambda \int g^2(r) dr + \iint g(x)g(y)\rho^{(2)}(x,y) dx dy, \quad (2)$$

where the factor 2 in front of the first term comes from the second moment of a unit-mean exponential RV modeling the fast fading, $\mathbb{E}\{h^2\} = 2$, and $\rho^{(2)}(x,y)$ in the second term describes the second-order properties of the distribution of vehicles, i.e., $\rho^{(2)}(x,y) dx dy$ is the probability that two vehicles are located in the infinitesimal regions dx, dy .

In order to calculate $I = \iint g(x)g(y)\rho^{(2)}(x,y) dx dy$ in equation (2), we note that the point process is stationary, thus the correlation function $\rho^{(2)}(x,y)$ depends only on the distance separation $|y-x|$. Since two vehicles are separated at least by the tracking distance, the correlation function becomes zero for distances smaller than c , i.e., $\rho^{(2)}(|y-x| \leq c) = 0$. When the distance separation lies between c and $2c$, no other vehicles can be located in-between. Therefore for $y > x$, $\rho^{(2)}(c \leq y-x \leq 2c) = \lambda\mu e^{-\mu(y-x-c)}$, where $\lambda\mu dx dy$ is the probability that two vehicles are located in the infinitesimal regions dx, dy , and $e^{-\mu(y-x-c)}$ is the probability that no other vehicle is located in $(x+c, y)$. For $y < x$, we just need to interchange x and y , thus $\rho^{(2)}(c \leq x-y \leq 2c) = \lambda\mu e^{-\mu(x-y-c)}$. When the distance separation lies between $2c$ and $3c$, at most one vehicle can be located between x and y , and the correlation function consists of two terms. For $y > x$, we get

$$\begin{aligned} \rho^{(2)}\left(2 \leq \frac{y-x}{c} \leq 3\right) &= \lambda\mu e^{-\mu(y-x-c)} + \lambda \int_{x+c}^{y-c} \mu e^{-\mu(z-x-c)} \mu e^{-\mu(y-z-c)} dz \\ &= \lambda\mu e^{-\mu(y-x-c)} + \frac{\lambda\mu^2(y-x-2c)}{e^{\mu(y-x-2c)}}, \end{aligned}$$

where $\mu e^{-\mu(z-x-c)} dz$ is the probability that a vehicle is located in the region dz centered at $z \in (x+c, y-c)$.

Following the same probability reasoning, when the distance lies between $3c$ and $4c$, there are at most two vehicles between x and y . The correlation function consists of three terms. The way to calculate the probabilities for at most one vehicle between x and y has been shown above. It remains to compute the probability there are two vehicles. For $y > x$, let us assume that the vehicles are located at z_1 and z_2 with $z_1 < z_2$. Then $z_1 \in (x+c, y-2c)$ and $z_2 \in (z_1+c, y-c)$. The probability that four vehicles are located at $x < z_1 < z_2 < y$ is

$$\lambda \int_{x+c}^{y-2c} \int_{z_1+c}^{y-c} \mu^3 e^{-\mu(z_1-x-c)} e^{-\mu(z_2-z_1-c)} e^{-\mu(y-z_2-c)} dz_2 dz_1.$$

After carrying out the integration above and summing up,

$$\rho^{(2)}\left(3 \leq \frac{y-x}{c} \leq 4\right) = \frac{\lambda\mu}{e^{\mu(y-x-c)}} + \frac{\lambda\mu^2(y-x-2c)}{e^{\mu(y-x-2c)}} + \frac{\lambda\mu^3(y-x-3c)^2}{2e^{\mu(y-x-3c)}}.$$

In a similar manner, we can compute the correlation function for larger distance separations. Finally, we get

$$\rho^{(2)}\left(k \leq \frac{y-x}{c} \leq k+1\right) = \lambda \sum_{j=1}^k \frac{\mu^j (y-x-jc)^{j-1}}{\Gamma(j) e^{\mu(y-x-jc)}}, k \geq 1. \quad (3)$$

The pair correlation in equation (3) has been studied in the context of statistical mechanics to describe the density variations of particles for one-dimensional hardcore fluids/gases as compared to the PPP, also known as the ideal, fluid/gas [22], [23]. The Laplace Tranform of (3) is available in [26, pp. 5].

In Fig. 2, we depict the normalized spatial correlation function. For small values of λc , the function decorrelates quickly. For increasing values of λc , the locations of pairs of vehicles remains correlated over larger distances. For $\lambda c = 1$, $\rho^{(2)}(x, y)$ becomes an infinite series of Dirac delta functions at $kc, k = 1, 2, \dots$; in that case, given the location of a vehicle, the locations of the rest of the vehicles become nonrandom.

After substituting equation (3) into the term I and doing some rearrangement we get

$$\begin{aligned} I &= 2\lambda \sum_{k=1}^{\infty} \int_{r_0}^{\infty} \int_{x+kc}^{x+(k+1)c} g(x)g(y) \sum_{j=1}^k \frac{\mu^j (y-x-jc)^{j-1}}{\Gamma(j) e^{\mu(y-x-jc)}} dy dx + \\ &\quad 2\lambda \sum_{k=1}^{\infty} \int_{r_0}^{\infty} \int_{x-(k+1)c}^{x-kc} g(x)G(y) \sum_{j=1}^k \frac{\mu^j (x-y-jc)^{j-1}}{\Gamma(j) e^{\mu(x-y-jc)}} dy dx \\ &= 2\lambda \sum_{k=1}^{\infty} \frac{\mu^k}{\Gamma(k)} \int_{r_0}^{\infty} \left(\int_{x+kc}^{\infty} g(x)g(y) \frac{(y-x-kc)^{k-1}}{e^{\mu(y-x-kc)}} dy + \right. \\ &\quad \left. \int_{-\infty}^{x-kc} g(x)G(y) \frac{(x-y-kc)^{k-1}}{e^{\mu(x-y-kc)}} dy \right) dx, \end{aligned} \quad (4)$$

where $G(y) = g(y)$ for $|y| \geq r_0$ and zero otherwise, and the factor 2 is added to account for $x \leq -r_0$.

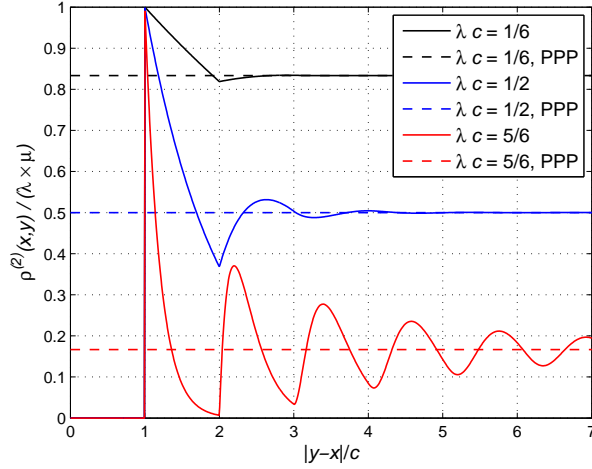


Fig. 2. Normalized correlation function $\frac{\rho^{(2)}(x,y)}{\lambda\mu}$ with respect to the normalized distance $\frac{|y-x|}{c}$ for different tracking distances c . The dashed lines correspond to $\rho^{(2)}(x,y) = \lambda^2$, or equivalently, $\frac{\rho^{(2)}(x,y)}{\lambda\mu} = 1 - \lambda c$.

For $c=0$, we get $\lambda=\mu$ and the term I in (4) degenerates to $\mathbb{E}\{\mathcal{I}\}^2$. For a positive $c>0$, the calculation of I is tedious because it involves double integration, an infinite sum and also it requires to filter out the vehicles associated with the cell of interest. Given a positive $r_0>0$ and $x>r_0$, the contributions to I for $y>x$ and $y<x$ are not equal. This is because for $y<x$, we need to exclude the vehicles inside the cell, giving rise to $G(y)$ instead of $g(y)$ in the integrand.

In order to simplify the calculation of I , we note that for increasing distance separation $|y-x|$, the correlation function becomes progressively equal to $\rho^{(2)}(x,y) \approx \lambda^2$. If we consider the exact expression of $\rho^{(2)}(x,y)$ for distances up to $2c$, and the PPP approximation of equal intensity for larger distances, the term I in (4) can be approximated as

$$I \approx 2\lambda\mu \int_{r_0}^{\infty} \left(\int_{x+c}^{x+2c} g(x)g(y) e^{-\mu(y-x-c)} dy + \int_{x-2c}^{x-c} g(x)G(y) e^{-\mu(x-y-c)} dy \right) dx + 2\lambda^2 \int_{r_0}^{\infty} \left(\int_{x+2c}^{\infty} g(x)g(y) dy + \int_{-\infty}^{x-2c} g(x)G(y) dy \right) dx. \quad (5)$$

After substituting (5) into (2), carrying out the integration describing the contribution to the second moment of interference from a single vehicle, and using that $\text{Var}\{\mathcal{I}\} = \mathbb{E}\{\mathcal{I}^2\} - \mathbb{E}\{\mathcal{I}\}^2$ we get

$$\text{Var}\{\mathcal{I}\} \approx \frac{4\lambda r_0^{1-2\eta}}{2\eta-1} - \mathbb{E}\{\mathcal{I}\}^2 + (5). \quad (6)$$

The accuracy of the above approximation for the standard deviation is illustrated in Fig. 3. Considering the exact correlation function for a larger range of distances, e.g., up to $4c$ will improve the model accuracy

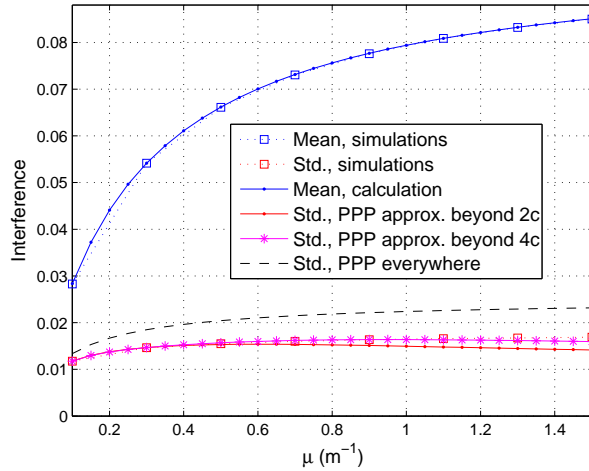


Fig. 3. Mean and standard deviation of interference with respect to the random part μ of the intensity of vehicles. Pathloss exponent $\eta=3$, and tracking distance $c=4$ m. Cell radius $r_0=50$ m. 100 000 simulation runs over a line segment of length 4 000 m. The integrals in (5), and similar integrals used to generate better approximation for the variance are evaluated numerically.

at the cost of computational complexity. Finally, note that if we ignore the hardcore properties of the point process and approximate the locations of vehicles using a PPP of intensity λ , i.e., $\rho^{(2)}(x, y) = \lambda^2 \forall (x, y)$, the associated variance is a rather loose upper bound to the variance of the point process.

We would like to capture the impact of tracking distance c on the variance of interference using a simple model. Assuming an intensity λ of vehicles, how does the variance due to a hardcore process, $c > 0$, scales as compared to the variance due to a PPP, $c=0$, of equal intensity? Equation (6) does not currently give much insight, mainly due to the complex nature of the term I in (5). In the next section, we capture the impact of parameters λ, c on the variance of interference, under the assumption of small tracking distances c as compared to the mean inter-vehicle distance λ^{-1} .

IV. CLOSED-FORM APPROXIMATION FOR THE VARIANCE

Let us consider the exact expression of the spatial correlation function $\rho^{(2)}(x, y)$ for distances up to $2c$, and the PPP approximation of equal intensity λ beyond that distance. This model does not introduce significant errors for small values of λc , i.e., small tracking distances as compared to the mean inter-vehicle distance, see also Fig. 2. The contribution to the second moment of interference due to pairs of

vehicles at distances larger than $2c$ is

$$\begin{aligned}
I_{>2c} &= 2\lambda^2 \left(\int_{r_0}^{\infty} \int_{x+2c}^{\infty} x^{-\eta} y^{-\eta} dy dx + \int_{r_0}^{\infty} \int_{-\infty}^{x-2c} x^{-\eta} G(y) dy dx \right) \\
&\stackrel{(a)}{=} \frac{1}{2} \mathbb{E}\{\mathcal{I}\}^2 + 2\lambda^2 \left(\int_{r_0}^{\infty} \int_{x+2c}^{\infty} x^{-\eta} y^{-\eta} dy dx + \int_{r_0+2c}^{\infty} \int_{r_0}^{x-2c} x^{-\eta} y^{-\eta} dy dx \right) \\
&= \frac{1}{2} \mathbb{E}\{\mathcal{I}\}^2 + \frac{2\lambda^2 r_0^{1-\eta}}{\eta-1} \left(\frac{(2c+r_0)^{1-\eta}}{\eta-1} + \frac{2cr_0^{-\eta}}{2\eta-1} {}_2F_1\left(\eta, 2\eta-1, 2\eta; -\frac{2c}{r_0}\right) \right) \\
&\stackrel{(b)}{=} \frac{1}{2} \mathbb{E}\{\mathcal{I}\}^2 + \frac{2\lambda^2 r_0^{2-2\eta}}{\eta-1} \left(\frac{(2b+1)^{1-\eta}}{\eta-1} + \frac{2b}{2\eta-1} {}_2F_1(\eta, 2\eta-1, 2\eta; -2b) \right),
\end{aligned} \tag{7}$$

where (a) follows from $2\lambda^2 \int_{r_0}^{\infty} \int_{-\infty}^{r_0} x^{-\eta} y^{-\eta} dy dx = \frac{1}{2} \mathbb{E}\{\mathcal{I}\}^2$, in (b) we substitute $b = \frac{c}{r_0}$, and ${}_2F_1$ is the Gaussian hypergeometric function [27, pp. 556].

For pair of vehicles at distance separation less than $2c$, we get contributions to the term I only for $c < |y-x| \leq 2c$ because $\rho^{(2)}(|y-x| \leq c) = 0$. The contribution to the second moment of interference due to pairs of vehicles at distances less than $2c$ and $y > x$ is

$$I_{<2c} \Big|_{y>x} = 2\lambda\mu \int_{r_0}^{\infty} \int_{x+c}^{x+2c} x^{-\eta} y^{-\eta} e^{-\mu(y-x-c)} dy dx. \tag{8}$$

After integrating in terms of y we get

$$I_{<2c} \Big|_{y>x} = 2\lambda\mu^{\eta} \int_{r_0}^{\infty} x^{-\eta} e^{\mu(c+x)} \left(\Gamma(1-\eta, (c+x)\mu) - \Gamma(1-\eta, (2c+x)\mu) \right) dx,$$

where $\Gamma(a, x) = \int_x^{\infty} t^{a-1} e^{-t} dt$ is the incomplete Gamma function.

We cannot express the above integral in terms of well-known functions. In order to approximate it, we expand the integrand around $\mu(x+c) \rightarrow \infty$. Note that for a fixed λ and $c > 0$, we get $\mu = \frac{\lambda}{1-\lambda c} > \lambda$. In addition, $(x+c) > r_0$. Therefore the expansion should be valid for $\lambda r_0 \gg 1$, i.e., the average number of vehicles within the cell $[-r_0, r_0]$ must be high. This assumption must hold true with our system set-up because the notion of tracking distance does not make much sense under light traffic conditions. After expanding the integrand up to the first-order term and carrying out the integration we get

$$\begin{aligned}
I_{<2c} \Big|_{y>x} &\approx 2\lambda \int_{r_0}^{\infty} x^{-\eta} (x+c)^{-\eta} \left(\frac{1-e^{-c\mu}}{\mu} + \frac{\eta(e^{-c\mu}(1+c\mu)-1)}{\mu^2(x+c)} \right) dx \\
&= \frac{2\lambda(1-e^{-c\mu}) {}_2F_1\left(\eta, 2\eta-1, 2\eta; -\frac{c}{r_0}\right)}{(2\eta-1) r_0^{2\eta-1}} + \frac{\lambda(e^{-c\mu}(1+c\mu)-1) {}_2F_1\left(2\eta, \eta+1, 2\eta+1; -\frac{c}{r_0}\right)}{\mu r_0^{2\eta}}.
\end{aligned} \tag{9}$$

The contribution to the second moment due to pairs of vehicles at distances between c and $2c$ and $y < x$ is

$$\begin{aligned}
I_{<2c}|_{x>y} &= 2\lambda\mu \int_{r_0}^{\infty} \int_{x-2c}^{x-c} x^{-\eta} G(y) e^{-\mu(x-y-c)} dy dx \\
&= 2\lambda\mu \left(\int_{r_0}^{\infty} \int_{-\infty}^{x-c} x^{-\eta} G(y) e^{-\mu(x-y-c)} dy dx - \int_{r_0}^{\infty} \int_{-\infty}^{x-2c} x^{-\eta} G(y) e^{-\mu(x-y-c)} dy dx \right) \\
&= 2\lambda\mu \left(\int_{r_0+c}^{\infty} \int_{r_0}^{x-c} x^{-\eta} y^{-\eta} e^{-\mu(x-y-c)} dy dx - \int_{r_0+2c}^{\infty} \int_{r_0}^{x-2c} x^{-\eta} y^{-\eta} e^{-\mu(x-y-c)} dy dx \right).
\end{aligned} \tag{10}$$

From the last equality in (10) and (8), we may deduce that $I_{<2c}|_{y>x} = I_{<2c}|_{x>y}$ for $r_0 \geq c$. The assumption, $r_0 \geq c$, is true for realistic cell sizes and traffic conditions. Finally, the variance of interference can be approximated by adding the contribution to the second moment from a single vehicle, $\frac{4\lambda r_0^{1-2\eta}}{2\eta-1}$, and the contributions due to pairs of vehicles, i.e., adding the terms $I_{>2c}$ in (7), $I_{<2c}|_{y>x}$ in (9) and $I_{<2c}|_{x>y} = I_{<2c}|_{y>x} = I_{<2c}$.

$$\mathbb{V}\text{ar}\{\mathcal{I}\} \approx \frac{4\lambda r_0^{1-2\eta}}{2\eta-1} + I_{>2c} + 2I_{<2c} - \mathbb{E}\{\mathcal{I}\}^2. \tag{11}$$

From the relation $\mu = \frac{\lambda}{1-\lambda c}$, we see that $\lambda c = 1$ corresponds to a lattice with inter-point distance $c = \lambda^{-1}$, while $\lambda c = 0$ corresponds to a PPP of intensity λ . We would like to study how the variance behaves as we start departing from the PPP by introducing positive tracking distance $c > 0$, while λ remains fixed. We start from the approximation of the term $I_{<2c}$ in (9), we substitute μ , and expand around $\lambda c \rightarrow 0$ up to the second-order term.

$$I_{<2c} \approx \lambda^2 c^2 \left(\frac{2r_0^{1-2\eta} {}_2F_1\left(2\eta-1, \eta, 2\eta, -\frac{c}{r_0}\right)}{(2\eta-1)c} - \frac{r_0^{-2\eta}}{2} {}_2F_1\left(2\eta, \eta+1, 2\eta+1, -\frac{c}{r_0}\right) \right). \tag{12}$$

Next, we substitute (7) and (12) in (11).

$$\begin{aligned}
\mathbb{V}\text{ar}\{\mathcal{I}\} &\approx \frac{4\lambda r_0^{1-2\eta}}{2\eta-1} + \frac{2\lambda^2 r_0^{2-2\eta}}{\eta-1} \left(\frac{(2b+1)^{1-\eta}}{\eta-1} + \right. \\
&\quad \left. \frac{2b {}_2F_1(\eta, 2\eta-1, 2\eta; -2b)}{2\eta-1} \right) - \frac{\mathbb{E}\{\mathcal{I}\}^2}{2} + \lambda^2 r_0^{2-2\eta} \times \\
&\quad \left(\frac{2b {}_2F_1(2\eta-1, \eta, 2\eta, -b)}{2\eta-1} - \frac{b^2 {}_2F_1(2\eta, \eta+1, 2\eta+1, -b)}{2} \right).
\end{aligned}$$

After expanding the above approximation up to the second order in $b = \frac{c}{r_0}$ we get

$$\mathbb{V}\text{ar}\{\mathcal{I}\} \approx \frac{4\lambda r_0^{1-2\eta}}{2\eta-1} (1 - \lambda c) + \lambda^2 c^2 r_0^{-2\eta}. \tag{13}$$

If we repeat the abovementioned procedure but considering the exact spatial correlation function up to distance $3c$ (instead of $2c$), and the PPP approximation beyond $3c$, we get

$$\mathbb{V}\text{ar}\{\mathcal{I}\} \approx \frac{4\lambda r_0^{1-2\eta}}{2\eta-1} \left(1 - \lambda c + \frac{\lambda^2 c^2}{2}\right) + \lambda^2 c^2 r_0^{-2\eta}. \quad (14)$$

The leading order term, $r_0^{1-2\eta}$, in (13) and (14), will dominate the variance of interference for $r_0 \gg c$. In addition, for small λc , we can use the expansion of the exponential function around zero, $e^{-\lambda c} \approx 1 - \lambda c + \frac{\lambda^2 c^2}{2}$, to get

$$\mathbb{V}\text{ar}\{\mathcal{I}\} \approx \frac{4\lambda r_0^{1-2\eta}}{2\eta-1} e^{-\lambda c}. \quad (15)$$

The above approximation gives a simple way to relate the variance of interference due to a PPP of intensity λ , with the variance of interference due to a hardcore process of equal intensity, assuming a small tracking distance c as compared to the mean inter-vehicle distance λ^{-1} . Introducing a tracking distance, while keeping the intensity of vehicles fixed, reduces the randomness in the deployment, and this reduction results in exponential reduction $e^{-\lambda c}$ for the variance of interference, or equivalently, $e^{-\frac{\lambda c}{2}}$, for the standard deviation.

In Fig. 4, we have simulated the standard deviation of interference for relatively high traffic conditions $\lambda = 0.1 \text{ m}^{-1}$, i.e., on average one vehicle every 10 m. We depict the results for $\lambda c \in (0, 0.8)$. We see that the closed-form models in (13), (14), and the exponential scaling of the variance of interference due to a PPP by $e^{-\lambda c}$, see (15), are indeed valid for small c . The model in (14) provides also a good fit for realistic tracking distances. This is because it uses the exact correlation function up to $3c$ instead of $2c$, and also, the expansion for the term $I_{<2c}$ around $\lambda c \rightarrow 0$, see (12), does not seem to introduce much error. In addition, the considered tracking distances, $c \in (0, 8)$ m are much smaller than the cell size r_0 , thereby the expansion around $\frac{c}{r_0} \rightarrow 0$ is accurate too. For tracking distances $c > 6$ m, we see that the model using the exact correlation function up to $2c$ starts to fail. This is because for a large c , the random part μ of the deployment becomes also high to maintain a fixed intensity λ . In that case, there is considerable correlation over distances larger than $2c$, and another model, e.g., the one using the exact correlation function up to $3c$, $4c$ and beyond would be needed.

In Fig. 5, we replicate the results of Fig. 4 but for lower traffic intensity, on average, one vehicle per 40 m. The average inter-vehicle distance becomes comparable to the cell size r_0 , and the feasible tracking distances can span a much larger range of values. We depict the results only up to $c = 25$ m, or equivalently $\lambda c \in (0, 0.625)$. We deduce from the figure that the models (13)–(15) do not fail due to the approximation of the correlation function for distances larger than $2c$. Also, we note that the source of error for large tracking distances is the approximation in $\frac{c}{r_0} \rightarrow 0$ rather than the expansion around $\lambda c \rightarrow 0$.

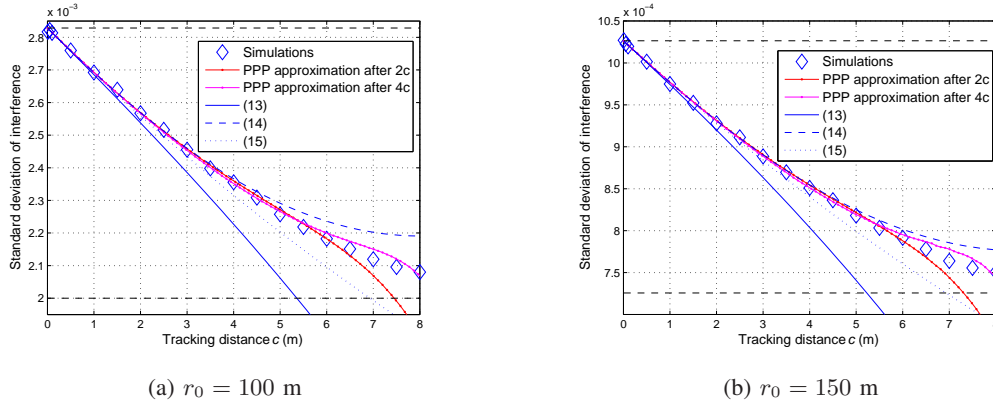


Fig. 4. Standard deviation of interference with respect to the tracking distance c . The intensity of vehicles is $\lambda = 0.1\text{m}^{-1}$. 2×10^5 simulation runs. Pathloss exponent $\eta=3$. For the 'PPP approximation after $2c$ ' we calculate $I_{>2c}$ from (7), and $I_{<2c}$ numerically from (8). The dashed line at the top corresponds to a PPP of intensity λ . The dashed line at the bottom corresponds to a lattice with inter-point distance λ^{-1} . The details for the calculation of the variance of interference due to a lattice are given in Section V.

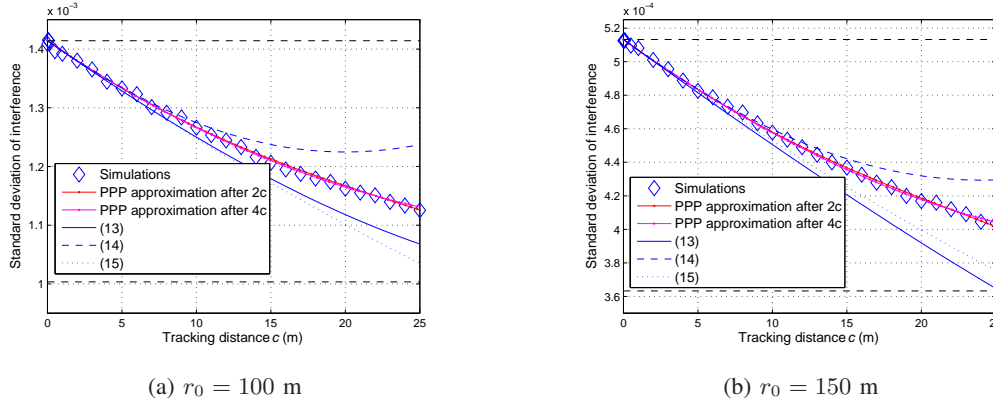


Fig. 5. Standard deviation of interference with respect to the tracking distance c . The intensity of vehicles is $\lambda = 0.025\text{m}^{-1}$. See the caption of Fig. 4 for parameter settings and explanation of the legends.

The models (13)–(15) are still valid for small tracking distances. Even for realistic tracking distances they give much more accurate predictions than a PPP model of equal intensity.

V. VARIANCE OF INTERFERENCE DUE TO A LATTICE

In the previous section, we gave some simple models approximating the variance of interference due to a hardcore process in terms of the variance of interference due to a PPP of equal intensity. The models are accurate for small tracking distances, and they also follow quite well the simulations for some realistic values. However, these models are constructed under the assumption of independent vehicle locations at

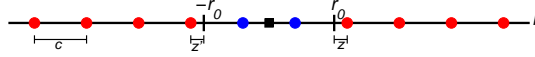


Fig. 6. One-dimensional lattice network. The base station, 'black square', is located at the origin. Interference is due to lattice points outside of the cell, 'red disks'. The RVs z, z' represent distances between the cell border and the lattice point nearest to it generating interference.

distance separation beyond $2c$, see (13), and $3c$, see (14). Therefore they cannot describe very accurately the interference due to the flow of platoons of vehicles, i.e., $\lambda c \rightarrow 1$. Due to its high complexity, we leave the study of this kind of flows for future work, and study the extreme scenario, $\lambda c = 1$, to get a preliminary insight. In this scenario, the locations of vehicles are modeled by a lattice. Some results about the statistics of interference generated from lattices can also be found in [28].

Besides Rayleigh fading, the source of randomness for lattice networks in our system set-up is the distance between the cell border and the nearest points to it generating interference, see Fig. 6. The instantaneous interference at the base station due to the lattice points located at the positive half-axis is

$$\mathcal{I} = \sum_{k=0}^{\infty} h_k g(x_k) = \sum_{k=0}^{\infty} h_k g(r_0 + z + kc),$$

where h_k, x_k is the fading coefficient and location for the k -th lattice point respectively, and z is a uniform RV, $z = U(0, c)$, describing the distance between the cell border r_0 and the nearest lattice point to it generating interference.

The moment generating function of interference is

$$\Phi_{\mathcal{I}}(s) = \iint e^{s\mathcal{I}} f_{\mathbf{h}} f_{\mathbf{x}} d\mathbf{h} d\mathbf{x},$$

where \mathbf{h}, \mathbf{x} are the vectors of fading coefficients and user locations respectively, and $f_{\mathbf{h}}, f_{\mathbf{x}}$ are the associated Probability Distribution Functions (PDFs).

The mean interference can be calculated by evaluating the first derivative of the moment generating

function at $s=0$.

$$\begin{aligned}
\mathbb{E}\{\mathcal{I}\} &= \left. \frac{\partial \Phi_{\mathcal{I}}}{\partial s} \right|_{s=0} \\
&= 2 \iint \sum_{k=0}^{\infty} h_k g(x_k) f_h f_x \mathrm{d}h \mathrm{d}x \\
&\stackrel{(a)}{=} 2 \iint \sum_{k=0}^{\infty} h_k g(r_0 + z + kc) f_h f_z \mathrm{d}h \mathrm{d}z \\
&\stackrel{(b)}{=} 2 \int \sum_{k=0}^{\infty} g(r_0 + z + kc) f_z \mathrm{d}z \\
&= \frac{2}{c} \int_0^c \sum_{k=0}^{\infty} (r_0 + z + kc)^{-\eta} \mathrm{d}z \\
&= \frac{2}{c^{1+\eta}} \int_0^c \zeta\left(\eta, \frac{r_0 + z}{c}\right) \mathrm{d}z,
\end{aligned} \tag{16}$$

where the factor 2 has been added to account for lattice points in the negative half-axis, (a) is due to the fact that given z , the locations of all points become nonrandom, (b) follows from independent fading coefficients and $\mathbb{E}\{h_k\}=1$, and $\zeta(n, x) = \sum_{k=0}^{\infty} (k+x)^{-n}$ is the Hurwitz Zeta function.

After carrying out the integration,

$$\mathbb{E}\{\mathcal{I}\} = \frac{2c^{-\eta}}{\eta-1} (\zeta(\eta-1, q) - \zeta(\eta-1, 1+q)) \stackrel{(a)}{=} \frac{2r_0^{1-\eta}}{c(\eta-1)}, \tag{17}$$

where in (a) we have used the identity for consecutive neighbors for the Hurwitz Zeta function $\zeta(n, x) = \zeta(n, 1+x) + x^{-n}$.

Note that due to the Campbell's Theorem [25], the mean interference can also be calculated by averaging the distance-based pathloss over the intensity (fixed) of points

$$\mathbb{E}\{\mathcal{I}\} = 2\lambda \int_0^{\infty} (r + r_0)^{-\eta} \mathrm{d}r = \frac{2\lambda r_0^{1-\eta}}{\eta-1},$$

where the intensity $\lambda = c^{-1}$.

In order to calculate the second moment of interference, we need to consider explicitly the interference originated from the negative half-axis since a scaling by 2 (as in the calculation of the mean) is not anymore valid. For that, we need first to identify the conditional Probability Mass Function (PMF) of the distance z' between the cell border $-r_0$ and the nearest lattice point to it generating interference, given the distance z , see Fig. 6. Let us denote $\epsilon = \frac{2r_0}{c} - \lfloor \frac{2r_0}{c} \rfloor$. The conditional PMF becomes equal to $z' = (c(1-\epsilon) - z)$ with probability $(1-\epsilon)$, and equal to $z' = (c(2-\epsilon) - z)$ with probability ϵ . For presentation clarity, we will assume in the derivation of the second moment of interference that the diameter of the cell, $2r_0$, is an integer multiple of the inter-point distance, i.e., $\epsilon = 0$. In that case, $z' = (c - z)$ with probability one. Extensions and numerical results for a positive ϵ will be given.

The second moment of interference can be calculated by evaluating the second derivative of the moment generating function at $s=0$

$$\begin{aligned}\mathbb{E}\{\mathcal{I}^2\} &= \left. \frac{\partial^2 \Phi_{\mathcal{I}}}{\partial s^2} \right|_{s=0} \\ &= \iint \left(\sum_{k=0}^{\infty} h_k g(x_k) + \sum_{m=0}^{\infty} h_m g(x_m) \right)^2 f_h f_x dh dx \\ &= \iint \left(2 \left(\sum_{k=0}^{\infty} h_k g(x_k) \right)^2 + 2 \sum_{k=0}^{\infty} \sum_{m=0}^{\infty} h_k h_m g(x_k) g(x_m) \right) f_h f_x dh dx,\end{aligned}$$

where the sum over m describes the interference from the lattice points in the negative half-axis, and the factor 2 in front of the square term is due to symmetry.

After expanding the square term we get:

$$\begin{aligned}\mathbb{E}\{\mathcal{I}^2\} &= \iint \left(2 \left(\sum_{k=0}^{\infty} h_k^2 g(x_k)^2 + \sum_{k=0}^{\infty} \sum_{k' \neq k} h_k h_{k'} g(x_k) g(x_{k'}) \right) + \right. \\ &\quad \left. 2 \sum_{k=0}^{\infty} \sum_{m=0}^{\infty} h_k h_m g(x_k) g(x_m) \right) f_h f_x dh dx \\ &\stackrel{(a)}{=} \int \left(2 \left(\sum_{k=0}^{\infty} 2g(x_k)^2 + \sum_{k=0}^{\infty} \sum_{k' \neq k} g(x_k) g(x_{k'}) \right) + \right. \\ &\quad \left. 2 \sum_{k=0}^{\infty} \sum_{m=0}^{\infty} g(x_k) g(x_m) \right) f_x dx \\ &\stackrel{(b)}{=} \underbrace{2 \int \sum_{k=0}^{\infty} g(x_k)^2 f_x dx}_{J_1} + \underbrace{2 \int \sum_{k=0}^{\infty} \sum_{k' \neq 0} g(x_k) g(x_{k'}) f_x dx}_{J_2} + \\ &\quad \underbrace{2 \int \sum_{k=0}^{\infty} \sum_{m=0}^{\infty} g(x_k) g(x_m) f_x dx}_{J_3},\end{aligned}$$

where (a) is due to $\mathbb{E}\{h_k^2\}=2$, $\mathbb{E}\{h_k\}=1$, and independent fading among the users, and in (b) we have added $k'=k$ in the second sum (so that the sum over k' goes over all positive integers similar to k) and subtract it from the first sum.

Recall that the distances z, z' to the cell borders are in general unequal $z \neq z'$. Therefore $J_2 \neq J_3$ because the sum over k' goes over the positive half-axis while the sum over m spans the negative half-axis. The term J_1 can be calculated as in equation (17), i.e., conditioning in terms of z , integrating the

Zeta function and using its consecutive neighbors identity

$$\begin{aligned}
J_1 &= 2 \int \sum_{k=0}^{\infty} g(r_0 + z + kc)^2 f_z dz \\
&= \frac{2}{c} \int_0^c \sum_{k=0}^{\infty} (r_0 + z + kc)^{-2\eta} dz \\
&= \frac{2c^{-2\eta}}{2\eta - 1} (\zeta(2\eta - 1, q) - \zeta(2\eta - 1, 1 + q)) \\
&= \frac{2\lambda r_0^{1-2\eta}}{2\eta - 1},
\end{aligned} \tag{18}$$

where $q = \frac{r_0}{c}$.

In a similar manner, the terms J_2 and J_3 can be expressed as

$$\begin{aligned}
J_2 &= \frac{2}{c} \int_0^c \sum_{k=0}^{\infty} \sum_{k'=0}^{\infty} (r_0 + z + kc)^{-\eta} (r_0 + z + k'c)^{-\eta} dz \\
&= 2c^{-2\eta-1} \int_0^c \zeta\left(\eta, \frac{r_0 + z}{c}\right)^2 dz. \\
J_3 &= \frac{2}{c} \int_0^c \sum_{k=0}^{\infty} \sum_{m=0}^{\infty} (r_0 + z + kc)^{-\eta} (r_0 + c - z + mc)^{-\eta} dz \\
&= 2c^{-2\eta-1} \int_0^c \zeta\left(\eta, \frac{r_0 + z}{c}\right) \zeta\left(\eta, \frac{r_0 + c - z}{c}\right) dz.
\end{aligned} \tag{19}$$

Note that for a positive ϵ , the calculation of J_1 , J_2 and J_3 requires to average over the PMF of distance z' . For positive ϵ , the terms J_1 and J_2 would also include integrals of sums over the negative half-axis; instead of scaling by 2 the corresponding integrals over the positive half-axis. Due to the fact that the RV z' is also uniform, $z' = U(0, c)$, similar to z , the calculation of J_1 and J_2 , after some manipulation, ends up being the same with equations (18) and (19). On the other hand, the term J_3 contains the cross-terms, over the positive and the negative half-axis, thus it requires to average over the conditional PMF of the RV z' given z . The term J_3 for $\epsilon > 0$ will give higher value as compared to the case with $\epsilon = 0$ in (19), reflecting the extra randomness introduced by the conditional PMF. Recall that for a arbitrary ϵ , $z' = ((1 - \epsilon)c - z)$ for $z \leq (1 - \epsilon)c$ and $z' = ((2 - \epsilon)c - z)$ for $z > (1 - \epsilon)c$. Therefore the term J_3 becomes

$$J_3 = \frac{2}{c^{2\eta+1}} \left(\int_0^{(1-\epsilon)c} \zeta\left(\eta, \frac{r_0 + z}{c}\right) \zeta\left(\eta, \frac{r_0 + c(1-\epsilon) - z}{c}\right) dz + \int_{(1-\epsilon)c}^c \zeta\left(\eta, \frac{r_0 + z}{c}\right) \zeta\left(\eta, \frac{r_0 + c(2-\epsilon) - z}{c}\right) dz \right). \tag{20}$$

Obviously for $\epsilon = 0$, equation (20) degenerates to the expression of J_3 in (19). Finally, the variance of interference can be read as

$$\mathbb{V}\text{ar}\{\mathcal{I}\} = \frac{2\lambda r_0^{1-2\eta}}{2\eta - 1} + J_2 + J_3 - \left(\frac{2\lambda r_0^{1-\eta}}{\eta - 1} \right)^2. \tag{21}$$

In Fig. 7, the integral-based calculation of the variance, see (21) with the term J_3 calculated in (20), is verified with the simulations. We include also the calculations with the term J_3 calculated in (19), i.e.,

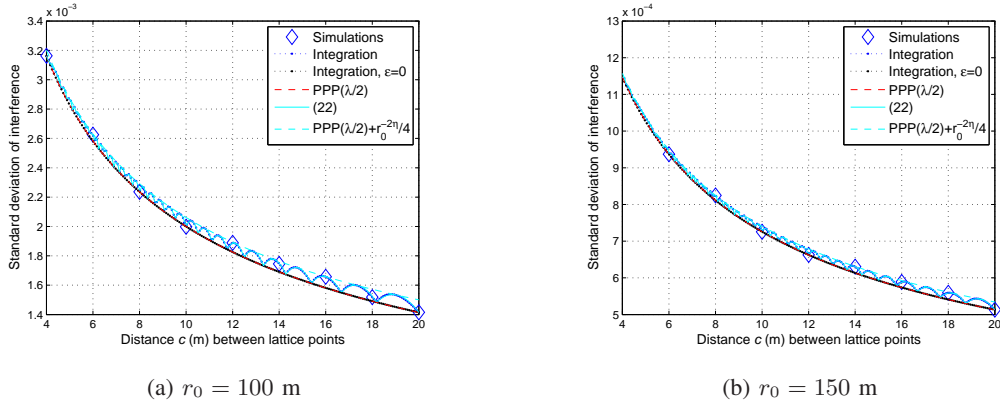


Fig. 7. Standard deviation of interference originated from a lattice. 5×10^6 simulation runs. Pathloss exponent $\eta = 3$. The integration corresponds to equation (21), where the terms J_2 in (19) and J_3 in (20) are evaluated numerically. The integration with $\epsilon = 0$ calculates J_3 numerically from (19). The standard deviation of interference due to a PPP of intensity $\frac{\lambda}{2}$ is $\sqrt{\frac{2\lambda r_0^{1-2\eta}}{\eta-1}}$, where $\lambda = c^{-1}$. The 'dashed cyan' line corresponds to $\sqrt{\frac{2\lambda r_0^{1-2\eta}}{\eta-1} + \frac{r_0^{-2\eta}}{4}}$.

neglecting the impact of randomness introduced by the RV z' , or equivalently, $\epsilon = 0 \forall \{c, r_0\}$. The impact of positive ϵ becomes more prominent for higher inter-point distance c while keeping the cell size r_0 fixed.

The integrals involved in the calculation of J_2 , J_3 are difficult to express in closed-form, see [29] for some recent work involving integrals of products of Zeta functions. In order to derive some closed-form approximation, we note that for a large $q = \frac{r_0}{c}$ and $\epsilon = 0$, the variance due to a lattice under Rayleigh fading can be well-approximated by the variance of the PPP of equal intensity scaled by $\frac{1}{2}$, i.e., $\frac{2\lambda r_0^{1-2\eta}}{2\eta-1}$. This is because the variance due to a PPP of intensity λ under Rayleigh fading, $\frac{4\lambda r_0^{1-2\eta}}{2\eta-1}$, accepts equal contributions, $\frac{2\lambda r_0^{1-2\eta}}{2\eta-1}$, due to fading and due to random user locations. The variance of interference due to a lattice with inter-point distance much less than the cell radius should be random only due to the fading, i.e., $\frac{2\lambda r_0^{1-2\eta}}{2\eta-1}$. In Fig. 7, we see that the corresponding curve due to a PPP of intensity $\frac{\lambda}{2}$ essentially overlaps with the curve depicting the integration-based results for a lattice with $c = \lambda^{-1}$ and $\epsilon = 0$. Their difference (not possible to notice it in the figure) is the standard deviation of interference due to a lattice in the absence of fading.

It might be useful to derive some closed-form approximation for the difference of the 'blue' and 'black' curves in Fig. 7. In this way, we can get an estimate about how much the interference due to a lattice can vary in terms of the parameter ϵ . In order to do that, we recall that it is only the term J_3 that depends on the parameter ϵ . Therefore we may expand J_3 for large q in equations (19) and (20), and take their difference. With large q , the argument of the Zeta function becomes also large, thus the Zeta function

can be well-approximated by an integral instead of a sum. Starting from equation (19) we get

$$\begin{aligned}
J_3 &= 2c^{-2\eta} \int_0^1 \zeta(\eta, q+x) \zeta(\eta, q+1-x) dx \\
&\approx 2c^{-2\eta} \int_0^1 \left(\int_0^\infty (k+q+x)^{-\eta} dk \int_0^\infty (k+q+1-x)^{-\eta} dk \right) dx \\
&= \frac{2c^{-2\eta}}{(\eta-1)^2} \int_0^1 (q+x)^{1-\eta} (q+1-x)^{1-\eta} dx \\
&\stackrel{(a)}{\approx} \frac{2c^{-2\eta}}{(\eta-1)^2} \int_0^1 \left(q^{1-\eta} - \frac{(\eta-1)x}{q^\eta} \right) \left(q^{1-\eta} - \frac{(\eta-1)(1-x)}{q^\eta} \right) dx \\
&= \frac{r_0^{-2\eta} \left(c^2 (\eta-1)^2 - 6c(\eta-1)r_0 + 6r_0^2 \right)}{3c^2 (\eta-1)^2},
\end{aligned}$$

where (a) uses that $q \gg x$ and does first-order expansion.

After doing, in a similar manner, first-order approximation for the term J_3 in (20) and subtract it from the above one, we get $\epsilon(\epsilon-1)r_0^{-2\eta}$. Therefore the variance of interference due to a lattice of inter-point distance c can be approximated as

$$\mathbb{V}\text{ar}\{\mathcal{I}\} \approx \frac{2\lambda r_0^{1-2\eta}}{2\eta-1} + \epsilon(1-\epsilon)r_0^{-2\eta}, \quad (22)$$

where the variance due to a lattice with $\epsilon=0$ has been approximated by the variance due to a PPP of intensity $\frac{\lambda}{2}$.

The accuracy of (22) is illustrated in Fig. 7, where it essentially overlaps with the integration-based results, 'blue' curve. Using $\epsilon=\frac{1}{2}$ in (22) indicates that under Rayleigh fading and large cell size, a lattice of intensity λ can at most increase by $\frac{r_0^{-2\eta}}{4}$ the variance of interference due to a PPP of intensity $\frac{\lambda}{2}$. This approximation is also available in Fig. 7. In Fig. 4 and Fig. 5, the selected values of cell size, r_0 , and intensity λ give $\epsilon=0$. We can also observe over there the approximately $\sqrt{2}$ -relation of the standard deviations of interference due to a PPP and a lattice of equal intensity under Rayleigh fading.

VI. CONCLUSIONS

In this paper, we have shown that introducing small tracking distance c (as compared to the mean inter-vehicle distance) in one-dimensional vehicular networks reduces the variance of interference exponentially $e^{-\lambda c}$ with respect to the variance due to a PPP of equal intensity λ . Assuming that the tracking distance is equal to the average length of a vehicle, the exponential correction factor makes sense to use particularly under high traffic conditions, large λ . We have also studied the extreme scenario of interference due to one-dimensional lattice networks to get some first insight into the problem of interference due to the flow of platoons of vehicles and/or interference at traffic jams. Under the assumptions of Rayleigh fading and large cell size r_0 in comparison with the inter-point lattice distance, we have shown that a PPP of intensity $\frac{\lambda}{2}$ can be used to get a first, yet accurate, approximation for the variance. Adding to it a

term $\frac{r_0^{-2\eta}}{4}$, independent of the inter-point lattice distance, can be used as an upper bound. The results of this paper can serve as a preliminary step before incorporating cell association and uplink power control schemes to study connection outage in cellular vehicular networks. Temporal and spatial aspects of interference in moving networks with more complex headway models is also a matter of future work.

REFERENCES

- [1] M. Haenggi *et. al.*, “Stochastic geometry and random graphs for the analysis and design of wireless networks”, *IEEE J. Selected Areas Commun.*, vol. 27, pp. 1029-1046, Sept. 2009.
- [2] Z. Gong and M. Haenggi, “Interference and outage in mobile random networks: Expectation distribution and correlation”, *IEEE Trans. Mobile Comput.*, vol. 13, pp. 337-349, Feb. 2014.
- [3] K. Koufos and C.P. Dettmann, “Temporal correlation of interference and outage in mobile networks over one-dimensional finite regions”, *IEEE Trans. Mobile Comput.*, vol. 17, pp. 475-487, Feb. 2018.
- [4] N. Miyoshi and T. Shirai, “A cellular network model with Ginibre configured base stations”, *J. Advances Applied Probability*, vol. 46, pp. 832-845, 2014.
- [5] M. Haenggi, “Mean interference in hard-core wireless networks”, *IEEE Commun. Lett.*, vol. 15, pp. 792-794, Aug. 2011.
- [6] G. Karagiannis *et. al.*, “Vehicular networking: A survey and tutorial on requirements, architectures, challenges, standards and solutions”, *IEEE Commun. Surveys and Tutorials*, vol. 13, no. 4, pp. 584-616, 2011.
- [7] J.P. Jeyaraj and M. Haenggi, “Reliability analysis of V2V communications on orthogonal street systems”, *IEEE Globecom Workshops*, 2017.
- [8] F. Baccelli and X. Zhang, “A correlated shadowing model for urban wireless networks”, in *Proc. IEEE Int. Conf. Comput. Commun. (INFOCOM)*, Hong Kong, Apr./May 2015, pp. 801-809.
- [9] E. Steinmetz, M. Wildemeersch, T. Quek and H. Wymeersch, “A stochastic geometry model for vehicular communication near intersections”, *IEEE Globecom Workshops*, 2015.
- [10] M.J. Farooq, H. ElSawy and M.-S. Alouini, “A stochastic geometry model for multi-hop highway vehicular communication”, *IEEE Trans. Wireless Commun.*, vol. 15, pp. 2276-2291, Mar. 2016.
- [11] V.V. Chetlur and H.S. Dhillon, “Coverage analysis of a vehicular network modeled as Cox Process driven by Poisson Line Process”, *available at* <https://arxiv.org/abs/1709.08577>, 2017.
- [12] C.-S. Choi and F. Baccelli, “An analytical framework for coverage in cellular networks leveraging vehicles”, *available at* <https://arxiv.org/abs/1711.09453>, 2017.
- [13] B. Błaszczyszyn, P. Mühlethaler and Y. Toor, “Stochastic analysis of Aloha in vehicular ad hoc networks”, *Annals of Telecommunications*, vol. 68, pp. 95-106, Feb. 2013.
- [14] Z. Tong H. Lu, M. Haenggi and C. Poellabauer, “A stochastic geometry approach to the modeling of DSRC for vehicular safety communication”, *IEEE Trans. Intell. Transport Syst.*, vol. 17, pp. 1448-1458, May 2016.
- [15] N.P. Chandrasekharamenon and B. Ancharev, “Connectivity analysis of one-dimensional vehicular ad hoc networks in fading channels”, *EURASIP J. Wireless Commun. and Networking*, 2012.
- [16] Highway Capacity Manual, Transportation Research Board, National Research Council, Washington, DC, 2000.
- [17] S. Yin *et.al.*, “Headway distribution modeling with regard to traffic status”, *IEEE Intell. Vehicles Symp.*, pp. 1057-1062, 2009.
- [18] A. Daou, “On flow within platoons”, *Australian Road Research*, vol. 2, no. 7, pp. 4-13, 1966.
- [19] I. Greenberg, “The log-normal distribution of headways”, *Australian Road Research*, vol. 2, no. 7, pp. 14-18, 1966.

- [20] R.J. Cowan, “Useful headway models”, *Transportation Research*, vol. 9, no. 6, pp. 371-375, Dec. 1975.
- [21] G. Yan and S. Olariu, “A probabilistic analysis of link duration in vehicular ad hoc networks”, *IEEE Trans. Intell. Transp. Syst.*, vol. 12, pp. 1227-1236, Dec. 2011.
- [22] Z.W. Salsburh, R.W. Zwanzig and J.G. Kirkwood, “Molecular distribution functions in a one-dimensional fluid”, *J. Chemical Physics*, vol. 21, pp. 1098-1107, Jun. 1953.
- [23] R.L. Sells, C.W. Harris and E. Guth, “The pair distribution function for a one-dimensional gas”, *J. Chemical Physics*, vol. 21, pp. 1422-1423, 1953.
- [24] T.D. Novlan, H.S. Dhillon and J.G. Andrews, “Analytical modeling of uplink cellular networks”, *IEEE Trans. Wireless Commun.*, vol. 12, pp. 2669-2679, Jun. 2013.
- [25] S.N. Chiu, D. Stoyan, W.S. Kendall and J. Mecke, *Stochastic geometry and its applications*. ISBN: 978-0-470-66481-0, 2013.
- [26] D.C. Mattis, *The many-body problem. An Encyclopedia of exactly solved models in one dimension*. World Scientific Publishing, 1993.
- [27] M. Abramowitz and I.A. Stegun. *Handbook of mathematical functions with formulas, graphs and mathematical tables*. 1972.
- [28] M. Haenggi, “Interference in lattice networks”, *available at* <https://arxiv.org/abs/1004.0027>, 2010.
- [29] M.A. Shopt, and R.B. Paris, “Integrals of products of Hurwitz zeta functions via Feynman parametrization and two double sums of Riemann zeta functions”, *available at* <https://arxiv.org/abs/1609.05658>.